International Journal of Solids and Structures 97–98 (2016) 389–399

Contents lists available at ScienceDirect

International Journal of Solids and Structures

journal homepage: www.elsevier.com/locate/ijsolstr

Toughening of thin ceramic plates using bioinspired surface patterns

Idris A. Malik, Francois Barthelat*

Department of Mechanical Engineering, McGill University, 817 Sherbrooke Street West, Montreal, QC H3A 2K6, Canada

ARTICLE INFO

Article history:
Received 22 March 2016
Revised 25 June 2016
Available online 7 July 2016

Keywords:
Bio-inspiration
Sutured materials
Fracture toughness
Ceramics
Laser engraving
Crack deflection

ABSTRACT

High-performance natural materials such as bone, teeth or mollusk shells contain a large volume fraction of minerals to generate stiffness and hardness. They are also packed with weak interfaces, which generate nonlinear deformations and channel cracks into powerful toughening configurations. As a result, these natural materials achieve simultaneous stiffness, hardness and toughness, which are properties which are mutually exclusive in engineering materials. Following these concepts, we have engraved trenches with controlled patterns and depth in thin plates of aluminum oxide. The trenches can guide propagating cracks, which we use to implement toughening mechanisms and unusual deformation mechanisms. We present fracture results on samples with transverse interfaces and sinusoidal interfaces. We also explore interlocking-jigsaw like interfaces, which dissipate the most energy and produce the highest toughness. These interfaces also profoundly change the way the material deform in tension, by introducing controlled non-linear deformations accompanied with geometric hardening and frictional pullout, in an otherwise all-brittle material.

© 2016 Elsevier Ltd. All rights reserved.

1. Introduction

Improving the properties of traditional engineering materials is an ongoing challenge. An interesting and promising source of inspiration is nature, which provides many examples of materials with unusual and attractive properties. For example bone, teeth or mollusk shells are hard biological materials which must prevent catastrophic fracture from fatigue, overloading or impacts. While these materials are weaker than our best engineering composite materials, they are much stronger and tougher than their base components, boasting amplifications of properties which are unmatched in manmade materials. In these materials, relatively high contents of minerals generate the stiffness, strength and hardness which are required for their function. Considering the high content of brittle minerals of these materials, they are also remarkably tough and they can therefore combine high stiffness, strength and toughness, properties which are mutually exclusive in traditional engineering materials (Ritchie 2011). As a universal strategy in these materials, the propagation of cracks is managed and prevented by the many weak interfaces they contain (Barthelat, et al. 2016; Barthelat 2015; Dunlop, et al. 2011; Fratzl, et al. 2004). For example, cracks are deflected and twisted by the weak cement lines in cortical bone, which is a major toughening mechanism in this material (Currey 2002; Koester, et al. 2008). In teeth, cracks propagating along the proteinaceous sheaths between the mineral enamel rods are channeled towards region where propagation is more difficult (Fig. 1a, (Bajaj, et al. 2010)). In nacre, the massive inelastic deformations of interfaces in a process zone around cracks dissipate large amounts of energy, which is the main toughening mechanisms in this material (Fig. 1b, (Barthelat and Rabiei 2011)). Mechanisms of crack deflection or deformation at the interfaces are governed by friction, unfolding of proteins, hydrogen bonds or electrostatic interactions at the molecular scale (Barthelat, et al. 2016). In turn, the architectures of the interfaces amplify their local response to generate inelastic deformation and fracture mechanisms at larger length scales, ultimately leading to unusual and attractive combinations of stiffness, strength and toughness. The morphology of the interfaces has a strong influence on their mechanical response. For example cement lines in bone, sheaths in tooth enamel and interfaces in nacre are wavy, which increases the resistance to sliding and pullout (Barthelat, et al. 2007). More extreme cases are also found in nature in the form of interlocked suture lines (Cohn, et al. 1991) as seen in ammonites (Li, et al. 2011) (Fig. 1c), osteoderms of turtle shells (Chen, et al. 2015; Dunlop, et al. 2011) (Fig. 1d), or the linking girdles of diatoms (Lin, et al. 2014a,b).

Hard biological materials may also be interpreted as architectured materials (Barthelat 2015), where stiff blocks with precise shapes and arrangement are bonded by weaker and more deformable interfaces (Brechet and Embury 2013; Dyskin, et al. 2001). The general concepts associated with this particular type of material are shown in Fig. 2. On a generic force-deformation plot,

* Corresponding author.
E-mail address: francois.barthelat@mcgill.ca (F. Barthelat).

http://dx.doi.org/10.1016/j.ijsolstr.2016.07.010
0020-7683/© 2016 Elsevier Ltd. All rights reserved.

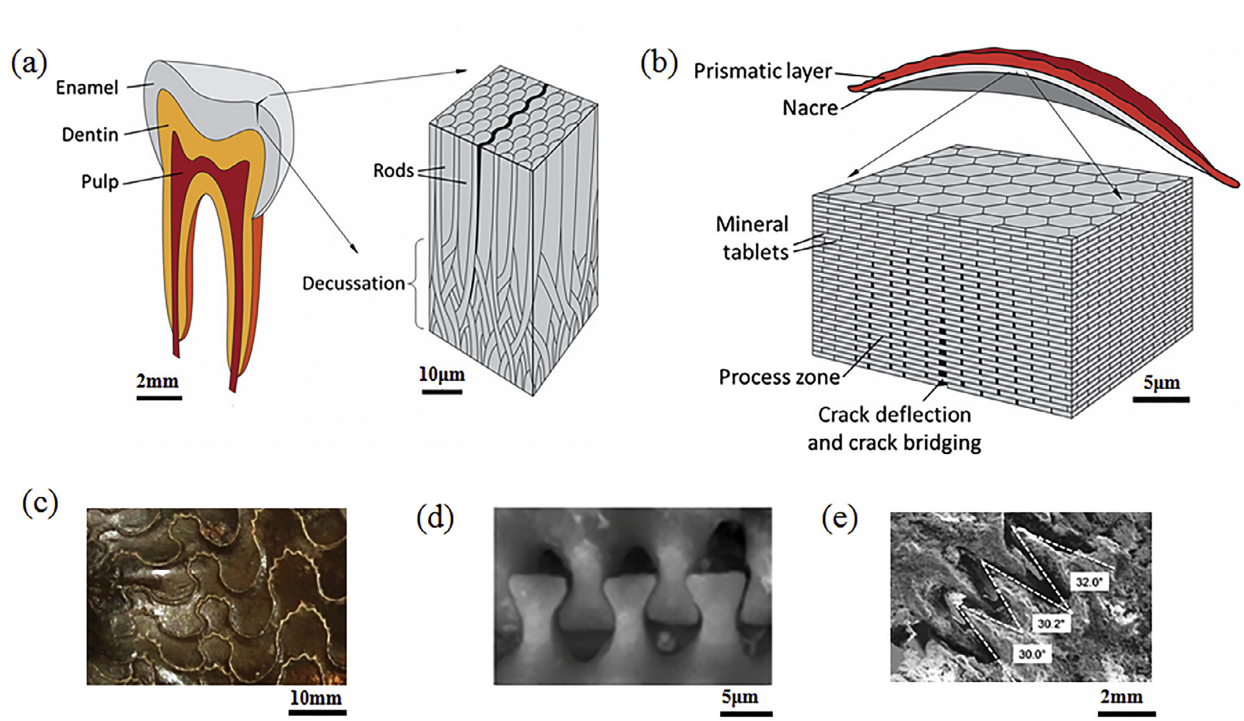

Fig. 1. (a) Overview of mammalian tooth and micro-architecture of enamel (adapted from Mirkhalaf, et al. (2014)); (b) overview of nacre and the toughening mechanisms (adapted from Mirkhalaf, et al. (2014)); Other natural system showing sutures: (c) *Ceratitic ammonoid* with intricate suture lines (Li, et al. 2011), (d) Linking girdles of diatoms (adapted from Lin, et al. (2014b)), and (e) Suture between osteoderms of a leather back sea turtle shell (adapted from Chen, et al. (2015)).

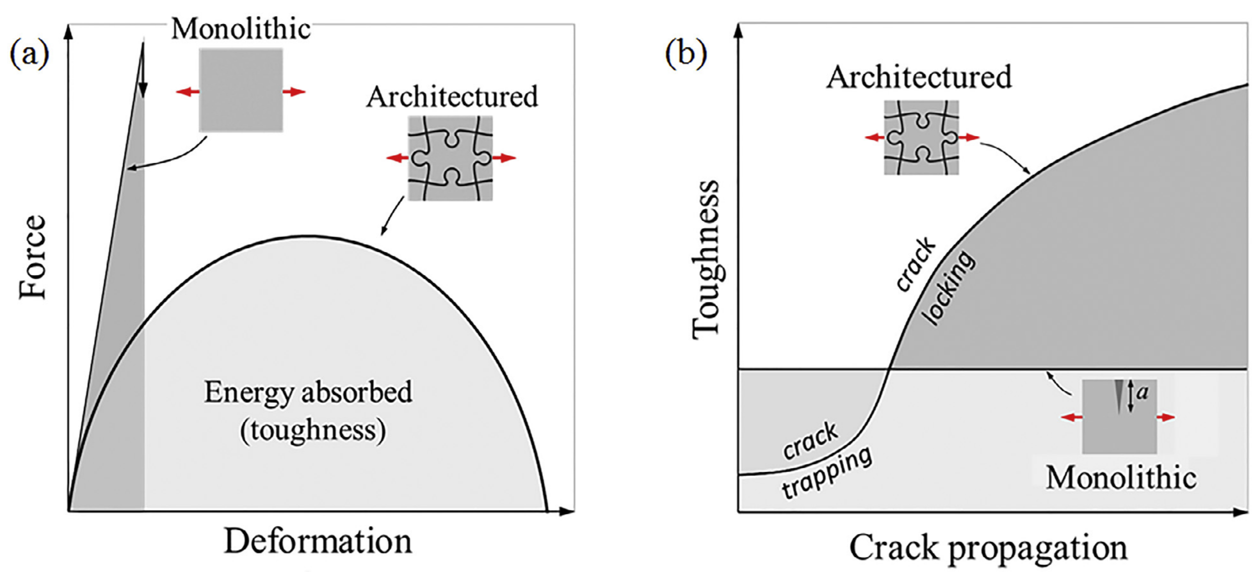

Fig. 2. General concepts in architectured materials for (a) large deformation and energy absorption, and (b) toughness (adapted from Mirkhalaf, et al. (2014)).

brittle materials deform linearly and fail at very small deformations (Fig. 2a). The addition of weak interfaces that can open (in mode I) or slide (in mode II) decreases the strength but increase overall deformation and energy absorption. Nonlinear deformations can spread over large volumes of material, from geometric hardening (Barthelat, et al. 2007), from strain hardening or from strain rate hardening at the interfaces (Chintapalli, et al. 2014; Tang, et al. 2007). In terms of fracture, a monolithic brittle material has a relatively low toughness which remains constant with crack extension (Fig. 2b). A material with weak interfaces will channel cracks along these interfaces which require these interfaces to be sufficiently weak compared to the bulk (Cook, et al. 1964; He and Hutchinson 1989; Parmigiani and Thouless 2006), with the implication that the initiation toughness is lower than the bulk material. However, with an adequate architecture, the cracks can be channeled into configurations that eventually impeded crack propagation, increasing the toughness to levels which are higher than the monolithic material (Fig. 2b). In this general description, the stiff but brittle material occupies 95–99% of the volume of the material as seen in nacre (Barthelat, et al. 2007), tooth enamel (Yahyazadehfar, et al. 2014) and other synthetic architectured materials (Mirkhalaf, et al. 2016).

The concept of weak interfaces carefully interspersed within materials is already used in engineering materials such as fiber

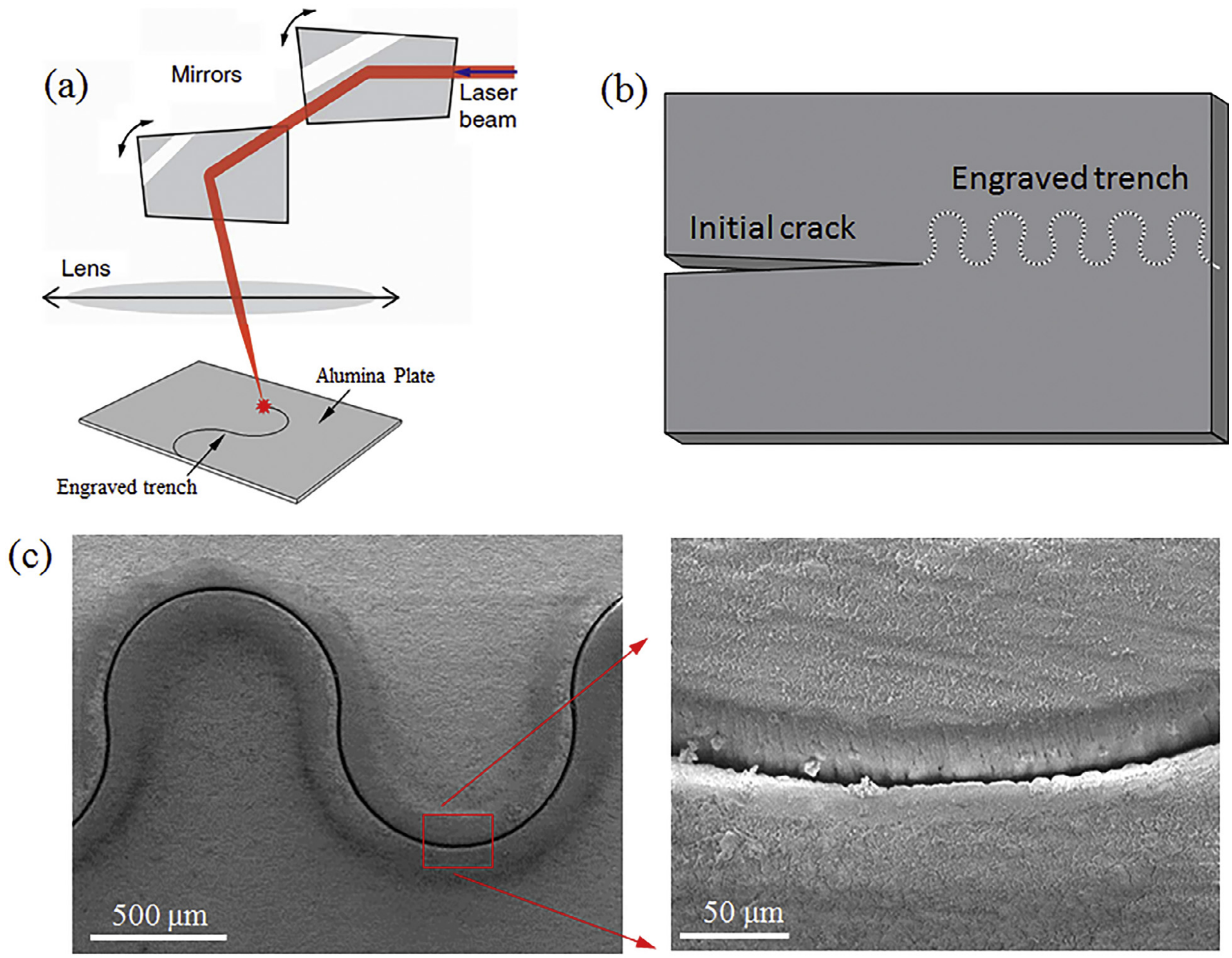

Fig. 3. (a) A 3D laser engraving set-up (b) a trench engraved ahead of a crack, in the shape of jigsaw line. (c) SEM images of a sample of the engraved alumina, showing the width of the trench.

reinforced composites (Evans 1989) and layered ceramics (Clegg, et al. 1990; Kovar, et al. 1998; Livanov, et al. 2015). However, the nature and morphology of the interfaces in these materials are far less sophisticated than what is observed in nature. Recently, we have implemented the idea of carving weak interfaces within the bulk of transparent glass to increase some of its mechanical properties, with emphasis on toughness and resistance to impacts (Mirkhalaf, et al. 2014). Here we use a laser engraving technique to carve a variety of well-controlled patterns of trenches on the surface of thin ceramic plates, providing weak interfaces that interact with incoming cracks, modify overall fracture toughness and in some cases completely transform the way this initially brittle material deforms and fails in tension.

2. Sample preparation

The base materials used in this study were 0.63 mm thick plates of nonporous, high-purity alumina (McMaster-Carr, IL, USA). Trenches with controlled patterns and depth were carved on the surface of the alumina using a laser engraver (Vitrolux, Vitro Laser solutions UG, Minden, Germany) to serve as guides for propagating cracks. The system uses a pulsed UV laser (355 nm, 500 mW cw pumped, 4 kHz repetition rate, 4–5 ns pulse duration) which is focused at a series of predefined points (Fig. 3a), ablating material from the surface of the ceramic plate to form a continuous trench. The pattern of the trench was created by the computer-controlled tilting of the laser beam with a set of mirrors, and the removal rate for the ceramic was adjusted by tuning the power of the laser and the spacing between the pulsed energy delivered by the laser (Tsai and Chen 2003; Yan, et al. 2013). The depth of the trench was controlled by the tuning of the removal rate and by the numbers of times the laser engraving was repeated on the same pattern.

Fig. 3b and c show an example of a pattern for the trench, in this case in the shape of an interlocking jigsaw-like suture. The spatial resolution of the pattern is high, the pattern of the trench on the ceramic perfectly matching the geometry of the desired pattern, with a uniform width of about 30 ms (Fig. 3c). The effects of the trenches on fracture toughness were evaluated using compact tension samples with the dimensions shown in Fig. 4a. The contours of the samples were cut from the plates. A 400 µm deep trench following the contour of the sample was first laser engraved, and a high-powered ultrasonicator with a flat ended probe (Sonics vibra cell, Sonics & Materials Inc., 53 Church Hill, Newtown CT USA) was then pressed directly onto the engraved trench. The probe transmitted high-frequency cyclic stress waves onto the sample, which propagated cracks from the engraved lines where the stresses were higher. This method of controlled fatigue crack propagation using ultrasonic stress waves is similar to experimental methods developed for the accelerated fatigue testing of materials (Mayer 1999). With our setup the cyclic stress waves applied to the material propagated fatigue cracks through the thickness, completely cutting the plate in about four minutes. The same method was used to prepare pin holes and the initial notch of the fracture samples.

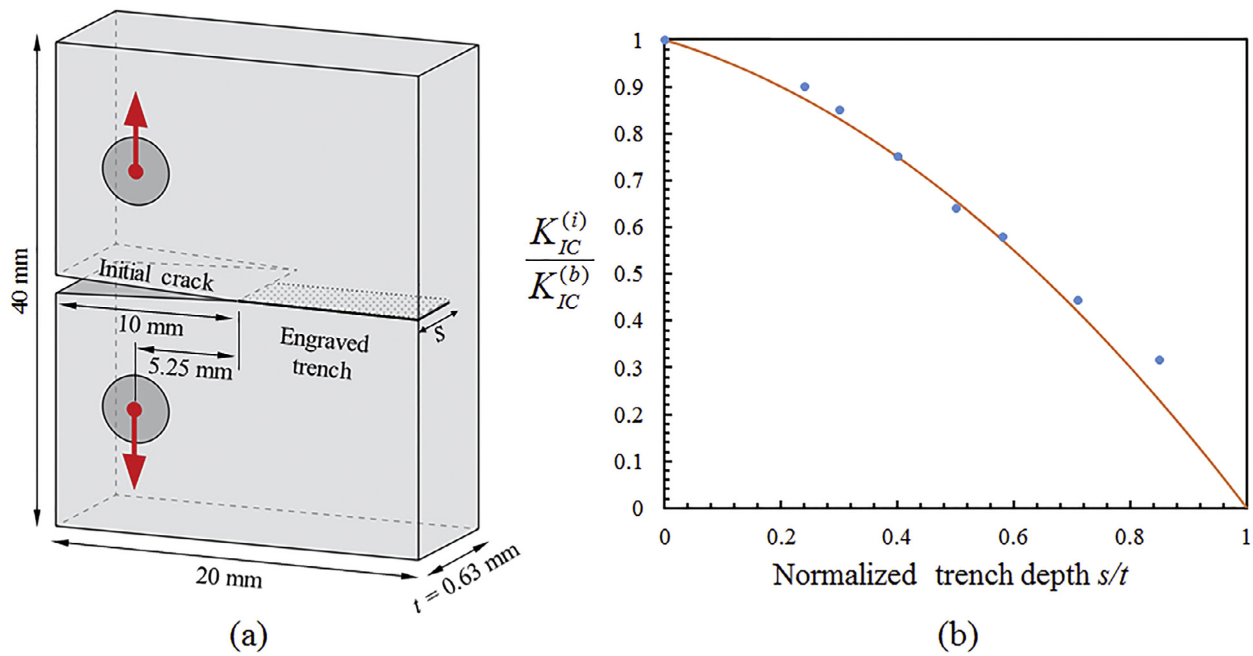

Fig. 4. (a) Schematic of the compact fracture sample with dimensions. In this case the sample contains a straight engraved trench ahead of the initial crack; (b) Effect of trench depth s (normalized by the plate thickness t) on the fracture toughness of the interface defined by the trench $K_{IC}^{(i)}$, normalized by the fracture toughness of the bulk ceramic $K_{IC}^{(b)}$.

3. Mechanical tests

The compact tension fracture samples and the tensile samples were tested using a miniature loading machine (Ernest F. Fullam Inc., Latham NY USA) at a displacement rate of $2\,\mu\text{ms}^{-1}$.

3.1. Tests on the bulk ceramic

The first series of tests was used to measure the toughness of the ceramic plate with no engraved trench. The force-deflection curve for the compact tension test sample was linear up to fracture which, as expected, was brittle. The maximum tensile force was used to compute the toughness of the ceramic using standard methods from linear elastic fracture mechanics with a compact tension configuration (ASTM 2005). A toughness of $K_{IC}^{(b)} = 5.04 \pm 0.06\,\text{MPa.m}^{1/2}$ ($N = 3$ samples) was found for the bulk ceramic, which is consistent with usual values for the toughness of aluminum oxide (Lawn 1993). This value served as a reference to assess the effect of various engraving patterns on overall toughness. We also measured the modulus and strength of the ceramic using a three-point bending configuration on small beams. We measured a modulus of about 355 GPa and a tensile strength of 365–395 MPa ($N = 2$ samples). The range of strength is approximate and we did not attempt a full characterization of the Weibull statistic for this material.

3.2. Fracture toughness of a straight engraved trench

The next series of tests was used to measure the apparent toughness of the engraved trench, and to assess the effect of its depth. We prepared and tested compact tension fracture samples which had exactly the same dimensions as the samples used to measure the toughness of the bulk ceramic, with the exception that these samples contained a straight engraved trench of controlled depth s ahead of the notch (Fig. 4a). Here and for the rest of this study, we were concerned with the apparent changes in toughness in reference to the bulk material, and we used the same standard methods to compute the fracture toughness of the engraved sample. All the samples discussed in Sections 3.2, 3.3 and 3.4 of this article failed in a brittle fashion, and possible local changes of stiffness or inelastic processes due to the engraved patterns were not considered when calculating toughness. We therefore assumed small scale yielding, where the state of stress at the crack tip is governed by a stress intensity factor K_I (the samples presented in Section 3.5 were analyzed differently). Fig. 4b shows the fracture toughness $K_{IC}^{(i)}$ of the interface formed by the engraved trench normalized by the fracture toughness of the intact plate $K_{IC}^{(b)}$, and as a function of the normalized depth of the trench s/t. The data shows how the effective toughness of the interface can be tuned to any value between the toughness of the bulk (i.e. $K_{IC}^{(i)} / K_{IC}^{(b)} = 1$, no trench), to zero (i.e $K_{IC}^{(i)} / K_{IC}^{(b)} = 0$, through cut) by adjusting the relative depth of the trench s/t. The laser engraving method therefore grants the ability to decrease the toughness of pre-defined lines that can deflect and guide propagating cracks within the plate. While the cracks can initially easily propagate along the weakened lines, carefully designed patterns can make crack propagation increasingly difficult. The cracks can therefore become progressively "trapped" as they propagate, which can effectively increase overall toughness by a significant margin.

3.3. Transverse interfaces

Crack deflection along weak interfaces is a well-known and powerful toughening mechanism for engineering and natural materials, including for ceramics and ceramic-ceramic composites (Clegg, et al. 1990; Kovar, et al. 1998; Livanov, et al. 2015). This strategy consists of creating weak interfaces across the expected crack path (which must be known a priori from the loading configuration of the component). The weak interfaces deflect propagating cracks transversely and away from the direction of the main driving force, which result in an overall increase of toughness (Clegg, et al. 1990; Cook, et al. 1964). In this study, we fabricated compact tension ceramic samples with a series of five straight trenches spaced by a distance $d = 10\,\text{mm}$ and oriented at 90° from the initial notch (Fig. 5a). The length of the trenches was varied using L_i

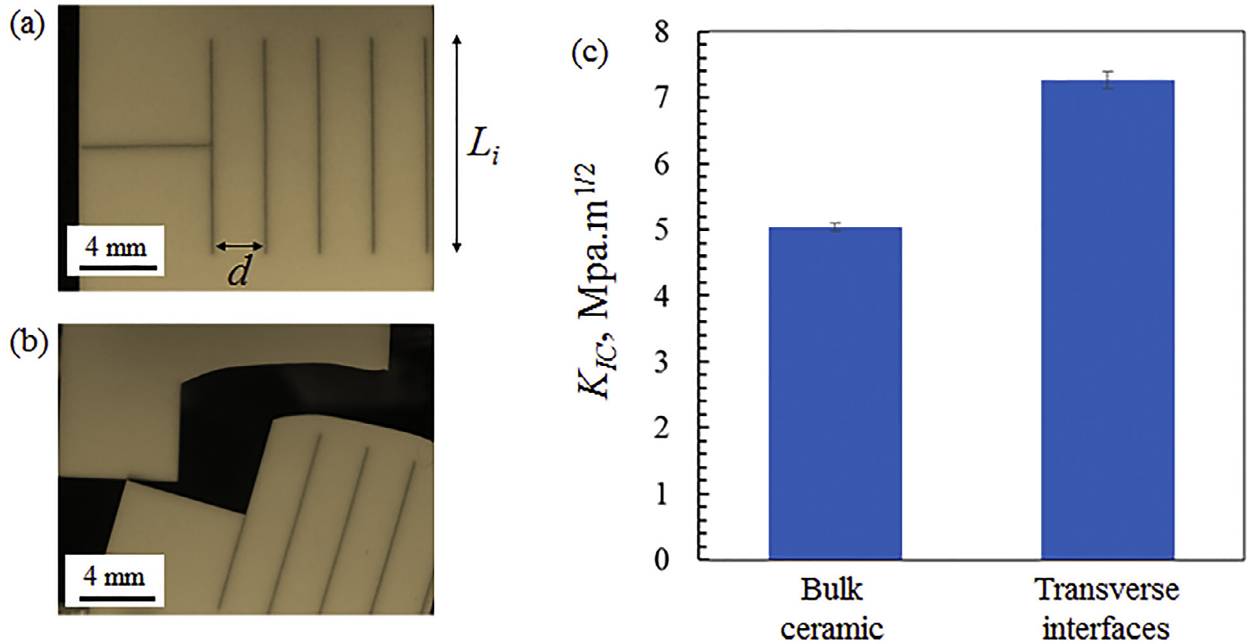

Fig. 5. Samples showing transverse trenches (a) initial sample (b) sample after testing. (c) Fracture toughness for bulk ceramic and ceramic with transverse interfaces. Data for the transverse interface is independent of d and L_i.

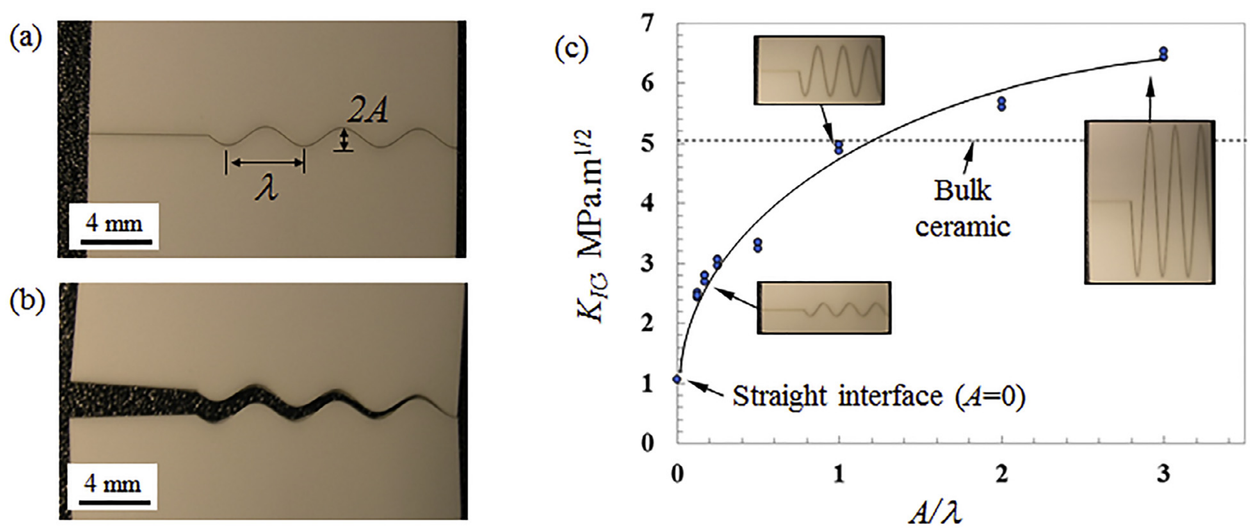

Fig. 6. Sinusoidal trench: (a) initial geometry showing amplitude and wavelength; (b) fractured sample; (c) Apparent fracture toughness of the interface as a function of the normalized amplitude of the pattern.

=12 mm, 18 mm and 22 mm. Preliminary tests showed that shallow trenches could not deflect the main crack. The crack could only be deflected for $s/t > 0.7$, corresponding to a relative interface toughness of $K_{IC}^{(i)}/K_{IC}^{(b)} < 0.45$ from our experimental calibration (Fig. 4b). A condition for crack deflection into a weak interface at 90° from crack propagation is $G_c^{(i)}/G_c^{(b)} < 1/4$, where $G_c^{(i)}$ and $G_c^{(b)}$ are the critical strain energy release rates for the interface and the bulk of the material, respectively (He and Hutchinson 1989). Setting aside the effects of fracture mode mixity as a coarse approximation, the condition can be written in terms of fracture toughness as $K_{IC}^{(i)}/K_{IC}^{(b)} < 1/2$. Our experimental observations on crack deflection are therefore in good agreement with theoretical predictions. In all cases, fracture of the samples was brittle, with no sign of stable crack propagation (upon fracture the force decreased sharply to zero). The crack followed the entire length of the engraved interface, after which the crack followed a horizontal trajectory parallel to the initial notch (Fig. 5b). Engraving transverse lines spanning the entire sample resulted in the sample completely splitting in the across direction. The apparent sample toughness was computed from the maximum force and reported on Fig. 5c. This toughness was about 45% higher than the bulk. The length of the engraved lines had no effect on this improvement, suggesting that the toughness improvement occurred upon crack initiation. A likely mechanism is the blunting of the initial crack by the engraved trench, a well-known mechanism described by Cook and Gordon (Cook, et al. 1964).

3.4. Wavy interfaces

The laser engraving method enables a large variety of patterns which are not necessarily based on straight lines. For example, recent models and experiments have shown that bond lines with a

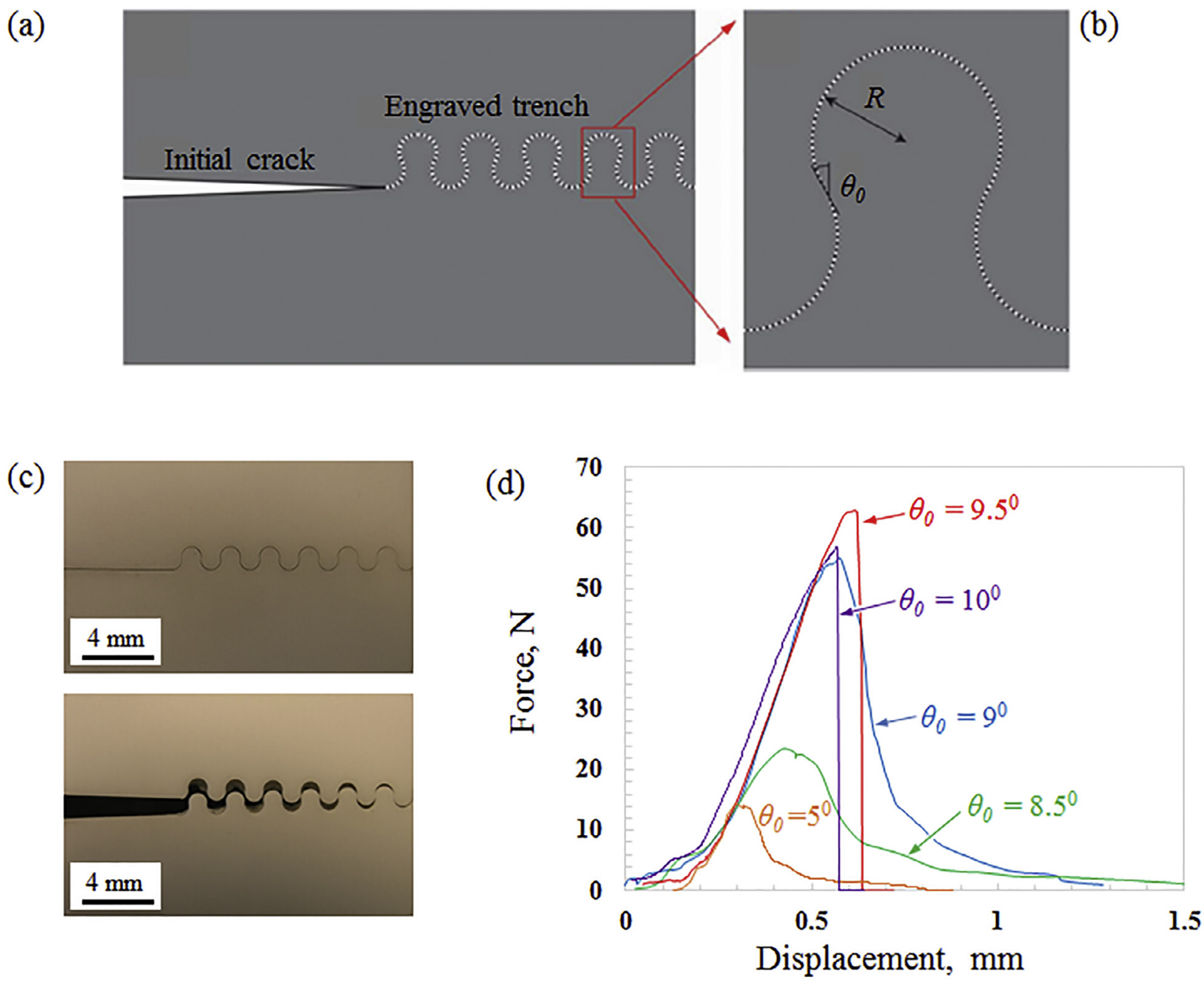

Fig. 7. Jigsaw-like trench: (a) configuration of the trench with respect to the initial crack; (b) individual jigsaw feature with geometrical parameters; (c) initial and fractured sample; (d) representative force-displacement curves for four locking angles.

wavy profile can increase toughness (Cordisco, et al. 2014; Zavattieri, et al. 2008a). In this study, we investigated sinusoidal interfaces in an all-ceramic system. A trench with a sinusoidal pattern of amplitude A and wavelength λ was engraved ahead of the notch, following the equation (Zavattieri, et al. 2008a):

$$y(x) = A\left(1 + \sin\left[2\pi\left(\frac{x}{\lambda} - \frac{1}{4}\right)\right]\right) \quad (1)$$

where x is the distance from the crack tip along the axis of the notch. Fig. 6a shows the geometry of the sinusoidal interface and its orientation with respect to the notch. The tip of the notch was positioned so the overall width of the suture (defined by the position of amplitude peaks) was centered on the line of the notch. This configuration was tested using a compact tension configuration, with a relative trench depth of $s/t = 0.75$. We examined the effect of A/λ by keeping λ at a constant value ($\lambda = 4$ mm) and by varying A ($A = 0.5$, 1, 2, 4, 8 and 12 mm). The engraved interface was weak enough to guide crack propagation along its entire length for all the values of A/λ that we tested here. The fracture was brittle, with no evidence of stable crack propagation or even short sequences of stable crack growth as previously reported for sinusoidal bond lines (Zavattieri, et al. 2008b). However, the fracture toughness of the sinusoidal trench increased with increasing amplitude, as shown in Fig. 6c. For $A/\lambda > 1$ the toughness of the interface became even greater than that of the bulk ceramic. When A/λ was increased further the data appeared to converge toward$K_{IC}/K_{IC}^{(b)} \approx 1.45$, which matches the improvement of toughness for transverse interfaces reported in the previous section (Fig. 5c). When $A/\lambda \rightarrow +\infty$, the section of the pattern encountered first by the propagating crack becomes close to a transverse line. As for the transverse interfaces, the mechanism of toughening for the sinusoidal line is also probably governed by crack blunting at the tip. Only the initial angle of the engraved line probably affected the initial fracture toughness measured experimentally. There was no evidence that the sinusoidal interface improved the stability of the crack, the force increasing linearly to a maximum value and then sharply dropping to zero upon crack propagation. Previous studies showed that a small amount of stable crack propagation is possible along wavy interfaces (Cordisco, et al. 2014; Zavattieri, et al. 2008a). However crack stability is, in general, function of both the material and the loading configuration (which includes sample geometry). It is likely that the configurations used in these previous studies (larger models, double cantilever beams) were more favorable to crack stability.

3.5. Jigsaw-like interlocking features

While the transverse and sinusoidal trenches could improve the fracture toughness of the bulk ceramic to some extent, crack stability was not improved. Here we explore the effect of re-entrant features on the trench line, designed to add stability and to dissipate

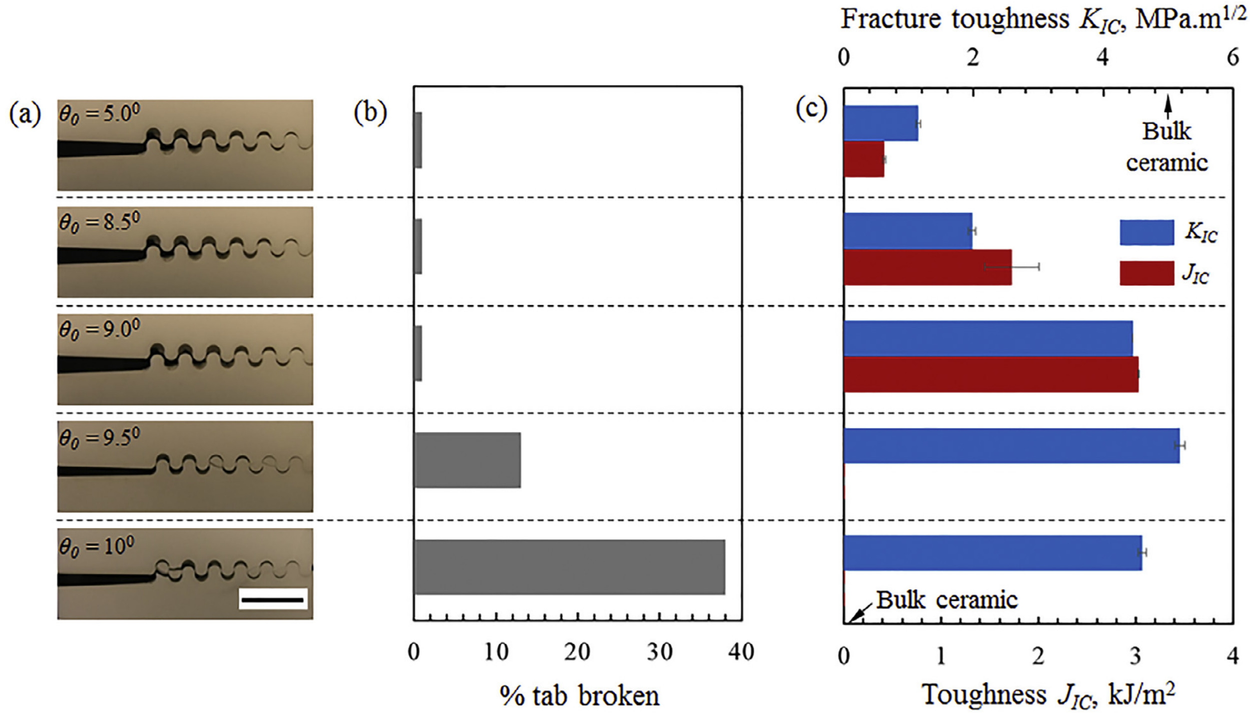

Fig. 8. (a) Pictures of fractured samples with increasing locking angle θ_0 (scale bar: 4 mm), (b) fraction of tabs broken during the test (c) maximum traction and toughness. For the cases $\theta_0 = 9.5°$ and $\theta_0 = 10°$ the fracture of the tab was extensive and J_{IC} was extremely small.

frictional energy upon pullout (Fig. 7a). This geometry, reminiscent from natural sutures in biological organisms (Li, et al. 2011), was previously implemented in thin glass slides where interlocking and frictional pullout significantly increased toughness (Mirkhalaf, et al. 2014). The geometry was constructed based on arcs of circles with radius R, joined to form a jigsaw-like feature with a locking angle θ_0 (Fig. 7b). Rounded features were used for the geometry in order to minimize stress concentrations in the ceramic. The radius was kept a constant value $R = 0.5$ mm, and different values of the locking angle were explored. Here we engraved jigsaw-like trenches of relative depth $s/t = 0.75$, and we then sonicated the engraved line in order to ensure that the pullout mechanisms prevailed over fracture of the ceramic. Fig. 7c show typical pictures of the engraved samples before and after testing. Opening the crack was a progressive and stable process which involved the pullout of the jigsaw-like tabs, with associated interlocking stresses and frictional dissipation. With the proper range of interlocking angles the pullout mechanism was successful, the system was stable and the force progressively decreased with crack opening. Fig. 7d shows representative force-displacement curves from the experiments. For angles $\theta_0 = 8.5°$ and $\theta_0 = 9°$, the force-deflection curves had a bell shape which is characteristic of tough, energy dissipating materials with stable crack growth. However, for $\theta_0 = 9.5°$ and higher, a large number of jigsaw-like tabs broke during the pullout process, and failure was more sudden and brittle-like.

The force-displacement curves were analyzed using two approaches. In the first approach, the maximum force was used to compute an apparent fracture toughness K_{IC}, using the same approach as in the previous sections. For the second approach, we computed J_{IC} as the area under the curve divided by the area of the fracture surface (obtained by multiplying the length of the ligament by the thickness of the sample). This second method is valid only when failure is progressive so that the energy given by the areas under the force-deflection curve corresponds to energy dissipated by the fracture process only. In the cases where failure was brittle, the area under the force-displacement curve includes dynamic effects which do not reflect the toughness of the material (Barinov 1993). Fig. 8 gives an overview of the results obtained for different locking angles. For small locking angle $\theta_0 \leq 9.0^0$ the samples failed entirely by the pullout of the tabs, and no damage of the tabs was observed (Fig. 8a,b). At higher locking angles some of the tabs broke in a brittle fashion, and in increasing numbers as the locking angle increased from 9.5^0 to higher values (Fig. 8a,b). Fig. 8c shows the fracture toughnessK_{IC} and toughness J_{IC} as function of locking angle. K_{IC} was computed from the maximum force as described above. J_{IC} was computed from the area under the force-deflection curve when the failure progressive. For the brittle cases, we used the standard relation$J_{IC} = K_{IC}^2/E$ where K_{IC} is the fracture toughness computed from the maximum force on the compact tension specimen and E is the Young's modulus for aluminum oxide ($E = 355$ GPa measured from experiments). With a Poisson's ratio of $\nu = 0.2$ typical of ceramics, the plane stress and plane strain version of this relation gave estimates for J_{IC} which were only a few percents apart. As the locking angle was increased, the fracture toughness increased to a maximum of $K_{IC} = 5.18 \pm 0.08$ MPa.m$^{1/2}$ at a locking angle $\theta_0 = 9.5^0$. At larger locking angles the toughness decreased, probably due to excessive damage in the tabs. Compared to the fracture toughness of the bulk ceramic ($K_{IC}^{(b)} = 5.04 \pm 0.06$ MPa.m$^{1/2}$), the gain in fracture toughness from the jigsaw-like pattern is therefore minimal. On the other hand, the gain in toughness in energy terms was significant. J_{IC} progressively increased with locking angle up to $\theta_0 = 9\ ^0$, at which $J_{IC} = 3.18$ kJ/m^2 which is about 45 times higher than the toughness of the bulk ceramic ($J_{IC}^{(b)} = 0.071$ kJ/m^2, computed from $K_{IC}^{(b)}$ and E). Samples with $\theta_0 = 9.5\ ^0$ and higher failed catastrophically, with a sharp decrease in J_{IC} (Fig. 8). The improvement in toughness generated by the jigsaw-like interfaces is the result of a fine tuning of the locking angle, as shown in Fig. 8. For small locking angles, the interlocking is minimal, frictional resistance is low, and as a result strength and toughness are also low. As the locking angle was increased interlocking increased, which translated in

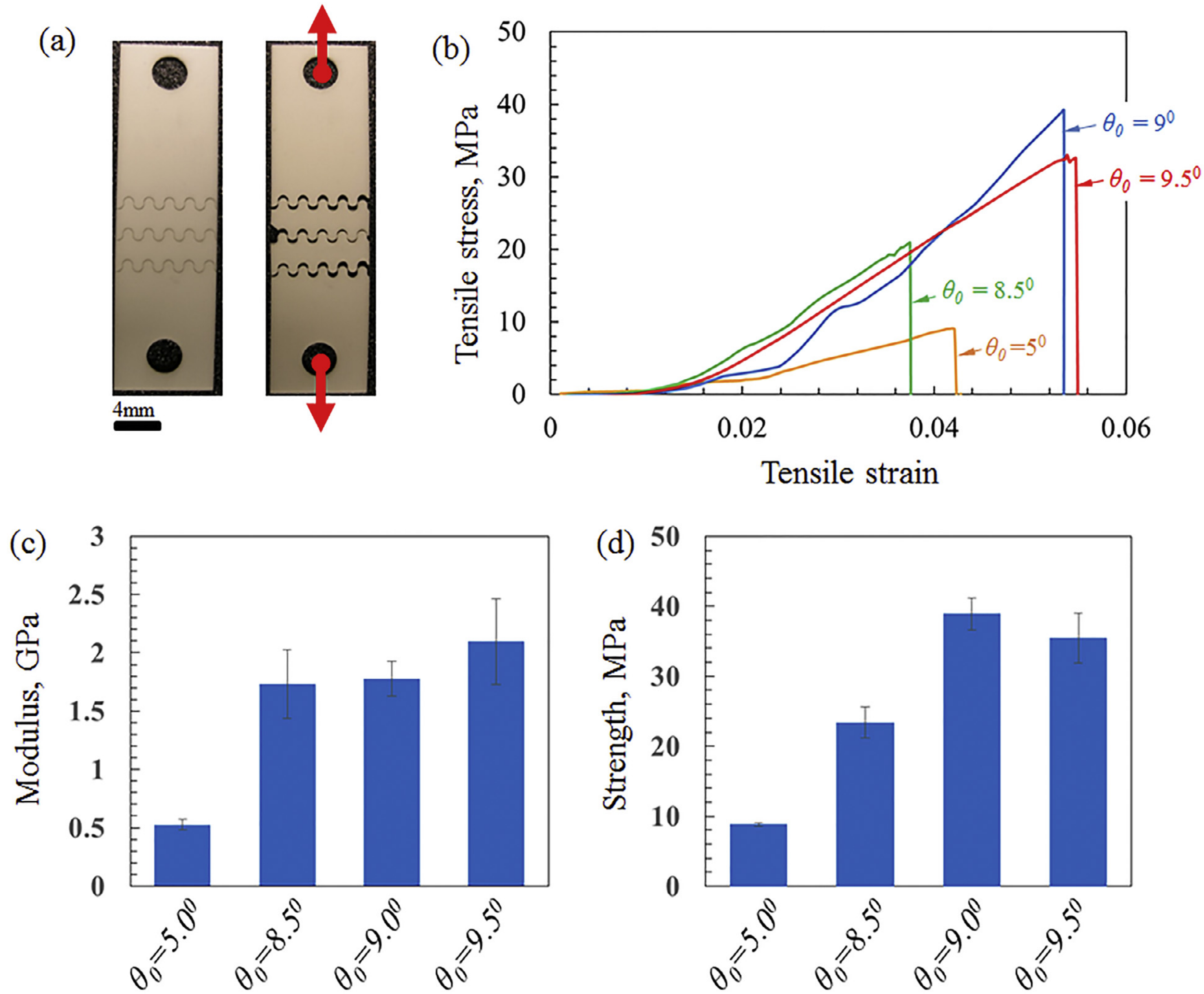

Fig. 9. (a) samples of tensile sample, before and during the test (b) stress-strain curve from the force-displacement curve of the tensile sample. Bar charts showing the (c) the maximum strength and (d) modulus of the engraved material with respect to the locking angle.

higher cohesive strength and higher toughness. However when the interlocking angle was too high the pullout process was prematurely interrupted by the fracture of the tabs, which resulted in decreased toughness. The optimum mechanical performance of the interface must therefore be finely tuned with the morphology of the suture, which is only possible with a fabrication method with very high spatial fidelity such as laser engraving.

We also evaluated the response of this material under uniaxial tensile loading. Tensile test samples were prepared in a similar fashion as those of the fracture samples, but with three jigsaw-like interfaces ($R = 0.5$ mm, $\theta_0 = 5^0$) spaced by a distance of 3 mm. Fig. 9b shows the corresponding tensile stress-strain curves. The curves show a low initial modulus characteristic of contact. The system then stiffens, and then progressively soften again as the jigsaw tabs completely pull apart. Remarkably, the geometric hardening associated with progressive interlocking is strong enough to spread non-linear deformations in all three engraved interfaces, although in some instances the edge of the sample broke off because of flexural stress from the pullout mechanism (Fig. 9a). The tabs of one of the three interfaces eventually completely pulled out and the sample fractured, which was marked by a sharp drop in the force. The strain at failure was in the order of 0.05, which is larger than the strain at failure of the monolithic ceramic by several orders of magnitude. Fig. 9b also shows that the stiffness and strength of the material increase as the locking angle is increased. Fig. 9c and d shows a summary of how these properties vary with locking angle. The modulus increase with locking angle in the range $\theta_0 = 5^0$–9.5^0. The tensile strength increased up to about 40 MPa for $\theta_0 = 9.0^0$, and then decreased for $\theta_0 = 9.5^0$ because of extensive damage to the tabs (Fig. 9c) resulting in prematurely interrupted pullout. Interestingly the variation of tensile strength measured across the samples we tested ($N = 3$ samples for each angle) was smaller than what is expected from a monolithic ceramic. This observation suggests that because of the failure mode of the architectured ceramic is very different from monolithic ceramics, their strength may not follow the traditional Weibull statistics. The engraving imparted the ceramic with completely different properties. It modulus was in the 2 GPa range (150 times less than the bulk ceramic), it strength in the 20–40 MPa range (depending on locking angle), which is about 10 times lower than the bulk ceramic. However its strain at failure was about 0.05, which is 50 times the strain at failure of bulk ceramic. The energy stored or absorbed in the material up to failure is also about four times higher in the architectured ceramic compared to the bulk ceramic.

4. Summary

High-performance biological materials such as bone, teeth or mollusk shells draw their high stiffness and hardness from high mineral content, and their toughness from their architecture

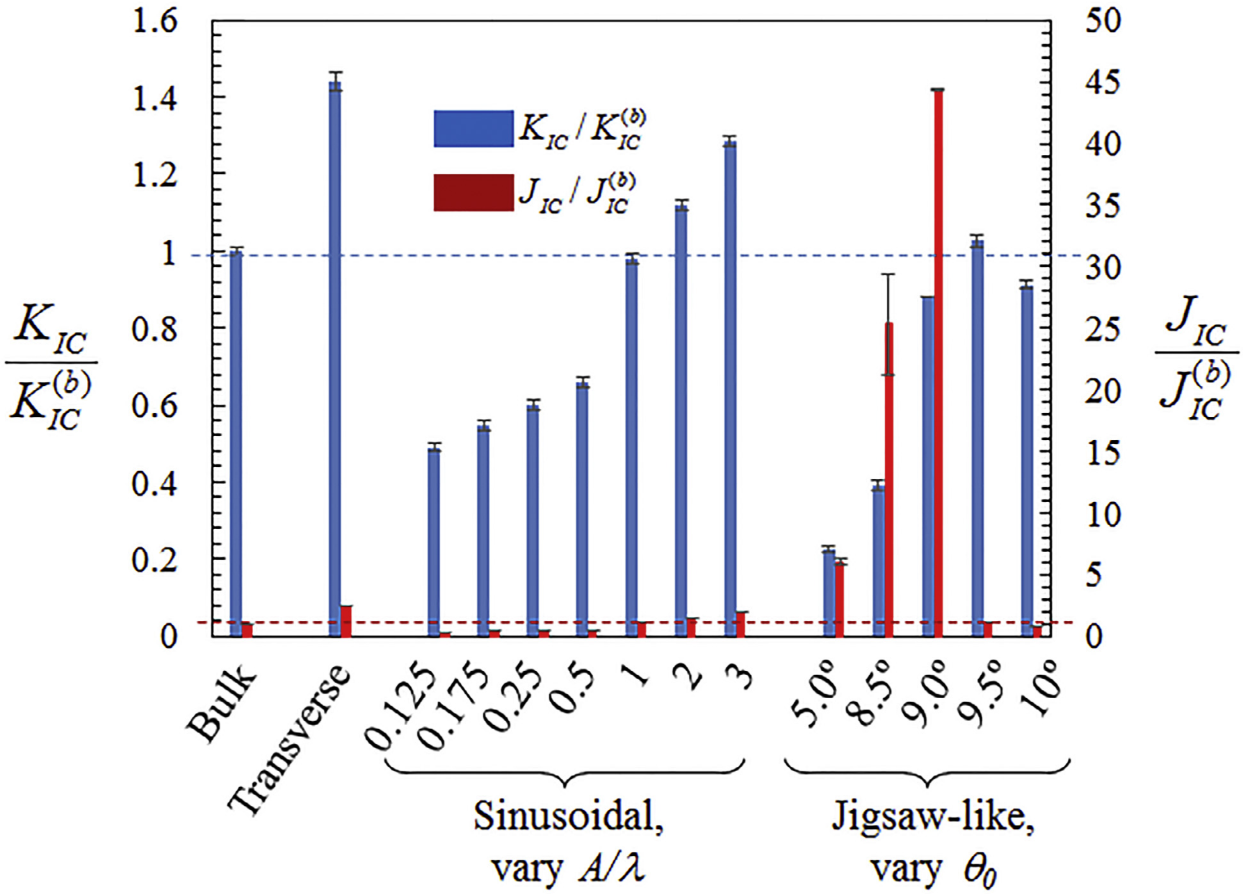

Fig. 10. Summary of the fracture toughness K_{IC} and toughness J_{IC} normalized by the properties of the bulk ceramic for transverse interfaces, sinusoidal interfaces and jigsaw-like interfaces.

(Barthelat 2015; Barthelat and Rabiei 2011). In particular, these materials contain weak interfaces with specific properties and arrangements which can deflect cracks and channel them into powerful toughening configurations (Barthelat, et al. 2016; Barthelat 2015; Dunlop, et al. 2011). Here we implemented these concepts in thin aluminum oxide plates. We engraved narrow trenches on thin plates of aluminum oxide, in order to guide cracks and to transform the way the material deforms and fracture. Our experiments show that crack deflection along transverse or sinusoidal interfaces can improve fracture toughness, but without any apparent added crack stability. A more potent geometry was a jigsaw-like suture with interlocking features, which can be adjusted through an interlocking angle. By finely tuning this angle we could make ceramics with high energy absorption capability and large deformability, but at the expense of modulus and strength. Fig. 10 shows a summary figure of the fracture toughness K_{IC} and toughness J_{IC} normalized by the properties of the bulk ceramic. The materials with the highest fracture toughness K_{IC} are not necessarily the materials with the highest toughness J_{IC}, and vice-versa. K_{IC} and J_{IC} are two measures of resistance to crack propagation that have different meanings. K_{IC} characterizes the resistance to crack propagation in terms of applied force, while J_{IC} characterizes the resistance to crack propagation in energy terms. In terms of applications and design, a material with a high K_{IC} will be able to resist crack propagation under a static load, while a material with a high J_{IC} will be able to resist crack propagation when subject to high amount of mechanical energy, as in the case of impact.

This work demonstrates that carefully introduced trenches can completely transform the mechanics and properties of thin ceramic plates. To maximize these properties and mechanisms a tight control over the morphology of the trenches is required, and we show that engraving with a focused laser beam is an ideal tool for this purpose. As opposed to glass where the focused laser is used to carve interfaces within the bulk of the materials (Mirkhalaf, et al. 2014; Mirkhalaf, et al. 2016), the ceramic we present here is opaque so only the surface was engraved. This approach is therefore the most effective on thin ceramic components, which could still have interesting and useful application in coatings for example. It is likely that the laser engraving process has little impact on the hardness, wear resistance and resistance to high temperatures of the base ceramic material we used (although we have not measured these properties in this work). Therefore potential applications include wear resistant or thermal barrier coatings, where some in-plane deformability of the hard coating could delay debonding from property mismatch with the substrate. In thicker ceramic, components failure often starts from the surface, because of the state of stress (bending, contact) and/or because of surface flaws. A possible extension of the method could examine the effect of engraving trenches on the surface of thick components such as flexural beams on their mechanical properties. The materials we present here show remarkable improvements in toughness, but at the expense of significant decreases in strength. Through further optimization and tuning is may however be possible to achieve higher strength. For example, the interactions between the tabs rely on frictional contact, which generate high stresses locally. The addition of a softer phase at the interface can redistribute stresses across the interfaces in order to prevent the fracture of the solid parts of the material. In turn, this improvement can open access to more extreme designs (for example, higher locking angles), which will translate into more favorable combinations of strength and toughness. Interfaces in hard biological materials are filled with proteins and/or polysaccharides, and some of these soft materials display unique and attractive molecular mechanisms of deformation with translate into added performance at the macroscale (Barthelat, et al. 2016). Filling the engraved trench of our ceramics with a second type of softer material could therefore provide additional dissipative mechanisms.

Acknowledgements

This work was supported by a Discovery Grant from the Natural Sciences and Engineering Research Council of Canada (NSERC). IAM was supported by a Scholarship from the Nigerian Government through the Nigerian Universities commission.

References

ASTM 2005. standard E399-05: Standard Test Method for Linear-Elastic Plane-Strain Fracture Toughness KIc of Metallic Materials.
Bajaj, D., et al., 2010. Fracture processes and mechanisms of crack growth resistance in human enamel. Jom 62 (7), 76–82.
Barinov, S.M., 1993. Work-of-fracture determination for brittle materials. J. Mater. Sci. Lett. 12 (9), 674–676.
Barthelat, F, Yin, Z, Buehler, M.J., 2016. Structure and mechanics of interfaces in biological materials. Nat. Rev. Mater. Appear.
Barthelat, F., 2015. Architectured materials in engineering and biology: fabrication, structure, mechanics and performance. Int. Mater. Rev. 60 (8), 413–430.
Barthelat, F., Rabiei, R., 2011. Toughness amplification in natural composites. J. Mech. Phys. Solids 59 (4), 829–840.
Barthelat, F., et al., 2007. On the mechanics of mother-of-pearl: A key feature in the material hierarchical structure. J. Mech. Phys. Solids 55 (2), 225–444.
Brechet, Y., Embury, J.D., 2013. Architectured materials: Expanding materials space. Scripta Materialia 68 (1), 1–3.
Chen, Irene H., Yang, Wen, Meyers, MarcA., 2015. Leatherback sea turtle shell: A tough and flexible biological design. Acta Biomaterialia 28, 2–12.
Chintapalli, RaviKiran, et al., 2014. Strain rate hardening: A hidden but critical mechanism for biological composites? Acta Biomaterialia 10 (12), 5064–5073.
Clegg, W.J., et al., 1990. A simple way to make tough ceramics. Nature 347 (6292), 455–457.
Cohn, M.B., Kim, C.J., Pisano, A.P., 1991. Self-assembling electrical networks: an application of micromachining technology. Solid-State Sensors and Actuators, 1991. In: 1991 International Conference on, 1991, pp. 490–493.
Cook, J., et al., 1964. A mechanism for the control of crack propagation in all-brittle systems. Proc. R. Soc. London A 282 (1391), 508–520.
Cordisco, Fernando, et al., 2014. On the mechanics of sinusoidal interfaces between dissimilar elastic–plastic solids subject to dominant mode I. Eng. Fract. Mech. 131, 38–57.
Currey, JohnD., 2002. Bones: Structure and Mechanics. Princeton University Press, Princeton, NJ.
Dunlop, J.W.C., Weinkamer, R., Fratzl, P., 2011. Artful interfaces within biological materials. Mater. Today 14 (3), 70–78.
Dyskin, A.V., et al., 2001. A new concept in design of materials and structures: Assemblies of interlocked tetrahedron-shaped elements. Scripta Materialia 44 (12), 2689–2694.
Evans, A.G., 1989. The mechanical performance of fiber-reinforced ceramic matrix composites. Mater. Sci. Eng. A 107 (C), 227–239.
Fratzl, P., Burgert, I., Gupta, H.S., 2004. On the role of interface polymers for the mechanics of natural polymeric composites. Phys. Chem. Chem. Phys. 6 (24), 5575–5579.
He, M.Y., Hutchinson, J.W., 1989. Crack deflection at an interface between dissimilar elastic materials. Int. J. Solids Struct. 25 (9), 1053–1067.
Koester, K.J., Ager III, J.W., Ritchie, R.O., 2008. The true toughness of human cortical bone measured with realistically short cracks. Nat. Mater. 7 (8), 672–677.
Kovar, D., Thouless, M.D., Halloran, J.W., 1998. Crack deflection and propagation in layered silicon nitride boron nitride ceramics. J. Am. Ceramic Soc. 81 (4), 1004–1012.
Lawn, B.R., 1993. Fracture of Brittle Solids. Cambridge University Press, New York.
Li, Yaning, Ortiz, Christine, Boyce, MaryC., 2011. Stiffness and strength of suture joints in nature. Phys, Rev. E 84 (6), 062904.
Lin, Erica, et al., 2014a. 3D printed, bio-inspired prototypes and analytical models for structured suture interfaces with geometrically-tuned deformation and failure behavior. J. Mech. Phys. Solids 73, 166–182.
Lin, Erica, et al., 2014b. Tunability and enhancement of mechanical behavior with additively manufactured bio-inspired hierarchical suture interfaces. J. Mater. Res. 29 (17), 1867–1875.
Livanov, K., et al., 2015. Tough alumina/polymer layered composites with high ceramic content. J. Am. Ceramic Soc. 98 (4), 1285–1291.
Mayer, H., 1999. Fatigue crack growth and threshold measurements at very high frequencies. Int. Mater. Rev. 44 (1), 1–34.
Mirkhalaf, M., Khayer Dastjerdi, A., Barthelat, F., 2014. Overcoming the brittleness of glass through bio-inspiration and micro-architecture. Nat. Commun. 5. http://www.nature.com/ncomms/2014/140128/ncomms4166/full/ncomms4166.html.
Mirkhalaf, M., Tanguay, J., Barthelat, F., 2016. Carving 3D architectures within glass: Exploring new strategies to transform the mechanics and performance of materials. Extreme Mech. Lett. 7, 104–113.
Parmigiani, J.P., Thouless, M.D., 2006. The roles of toughness and cohesive strength on crack deflection at interfaces. J. Mech. Phys. Solids 54 (2), 266–287.
Ritchie, RobertO., 2011. The conflicts between strength and toughness. Nat. Mater. 10 (11), 817–822.
Tang, H., Barthelat, F., Espinosa, H.D., 2007. An Elasto-Viscoplastic Interface Model for Investigating the Constitutive Behavior of Nacre. J. Mech. Phys. Solids. in press (available online January 2007).
Tsai, Chwan-Huei, Chen, Hong-Wen, 2003. Laser cutting of thick ceramic substrates by controlled fracture technique. J. Mater. Process. Technol. 136 (1–3), 166–173.
Yahyazadehfar, M., et al., 2014. On the mechanics of fatigue and fracture in teeth. Appl. Mech. Rev. 66 (3), 1–19.
Yan, Yinzhou, et al., 2013. CO2 laser high-speed crack-free cutting of thick-section alumina based on close-piercing lapping technique. Int. J. Adv. Manufact. Technol. 64 (9-12), 1611–1624.
Zavattieri, PabloD., Hector Jr, LouisG., Bower, AllanF., 2008a. Cohesive zone simulations of crack growth along a rough interface between two elastic–plastic solids. Eng. Fract. Mech. 75 (15), 4309–4332.
Zavattieri, PabloD., Hector Jr., LouisG., Bower, AllanF., 2008b. Cohesive zone simulations of crack growth along a rough interface between two elastic-plastic solids. Eng. Fract. Mech. 75 (15), 4309–4332.

Idris A Malik, is a PhD student at the laboratory of advanced materials and bioinspiration, department of Mechanical engineering, McGill University. He obtained a Bachelor's degree in Mechanical engineering from Ahmadu Bello University, Nigeria in 2010 and obtained a Master's degree in Petroleum engineering from African university of science and technology in 2013 before proceeding to McGill University for PhD in Mechanical engineering.

Francois Barthelat is an Associate Professor in the department of Mechanical Engineering, McGill University, Canada. He obtained is Bachelor's degree from École Nationale Supérieure d'électricité et de Mécanique (France), and Master degree in Mechanical Engineering from University of Rochester, and PhD in Mechanical Engineering from Northwestern University. He had authored several journal papers with focus on the mechanical performance of hard biological materials and development of novel bioinspired materials.